

Expanded Pharmacokinetic model for population studies in Breast MRI

Vandana Mohan^{a,b} Yoshihisa Shinagawa^b Bing Jian^b Gerardo Hermosillo^b

^aElectrical and Computer Engineering, Georgia Institute of Technology, Atlanta, GA

^bSiemens Medical Solutions USA, IKM CKS, Malvern PA

ABSTRACT

We propose a new model for pharmacokinetic analysis based on the one proposed by Tofts. Our model both eliminates the need for estimating the Arterial Input Function (AIF) and normalizes analysis so that comparisons across patients can be performed. Previous methods have attempted to circumvent the AIF estimation by using the pharmacokinetic parameters of multiple reference regions (RR). Viewing anatomical structures as filters, pharmacokinetic analysis tells us that 'similar' structures will be similar filters. By cascading the inverse filter at a RR with the filter at the voxel being analyzed, we obtain a transfer function relating the concentration of a voxel to that of the RR. We show that this transfer function simplifies into a five-parameter nonlinear model with no reference to the AIF. These five parameters are combinations of the three parameters of the original model at the RR and the region of interest. Contrary to existing methods, ours does not require explicit estimation of the pharmacokinetic parameters of the RR. Also, cascading filters in the frequency domain allows us to manipulate more complex models, such as accounting for the vascular tracer component. We believe that our model can improve analysis across MR parameters because the analyzed and reference enhancement series are from the same image. Initial results are promising with the proposed model parameters exhibiting values that are more consistent across lesions in multiple patients. Additionally, our model can be applied to multiple voxels to estimate the original pharmacokinetic parameters as well as the AIF.

1. INTRODUCTION

The diagnosis of breast cancer from Magnetic Resonance Imaging (MRI) data is a tough problem exacerbated by the fact that a malignant lesion often displays intensity patterns similar to benign tissues and other structures (such as the heart) in the field of view. However, malignant tissues differ from benign tissues in how Contrast Agents (CA) flow in and leak out. These molecules affect the observed intensity patterns because they change the longitudinal relaxation times at the voxels in the image. Unlike their behaviour with respect to intensity itself, malignant tissues display a characteristic pattern with regard to how much of the CA they take up, and also with regard to the rates of entry and washout of the CA. Dynamic Contrast-Enhanced (DCE) MRI uses this property to identify regions of interest. Pharmacokinetic (PK) analysis then aims to quantify the washin and washout of the CA towards differentiating malignant and benign lesions. The ideal goal of PK analysis in the context of breast MRI is to provide a framework where the kinetics of the CA within the tissue of interest can be quantitatively described, and compared across data sets from one or more patients and/or MR systems. However, current systems do not meet this requirement due to difficulties in the normalization that the system can perform on the input image data, which impairs the effectiveness of any population studies conducted.

Existing literature on Pharmacokinetic analysis for breast MR can be categorized into two broad classes of models - compartmental and heuristic. The first class attempts to describe the microscopic view of the breast tissues as a set of compartments and then models the interaction between these compartments with respect to the entry and exit of the CA. Within this class, the models differ in the number of compartments they use to model the tissue and the equations that describe the interactions. Heuristic models attempt to model the washin and washout phenomena - as growing(/decaying) exponentials for example - and quantify the extents and rates of the same. Of the compartmental models, the Tofts model is the most commonly used. This is the starting model from which the proposed model is derived. A comparative

study of different pharmacokinetic models for DCE-MRI can be found, for example in [4]. The challenges in estimating the quantity of CA in the vascular space and the unsatisfactory normalization which impairs population studies are the key issues that the proposed framework aims to address.

2. PREVIOUS WORK

2.1. Tofts model

The proposed model uses the Tofts two-compartment model [5] to describe the concentration at each voxel within the image with respect to the true AIF. By applying the idea of a reference region, it uses the expressions at two different voxels towards analytically eliminating the AIF from the analysis.

The Tofts model is a simplified model that considers the tissue of interest as one compartment (Extravascular Extracellular Space or EES) and everything extraneous to it as another compartment (Plasma) and models the kinetics of the contrast agent as an exchange between the two. The cells are not included in either of these compartments because by the nature of the contrast agents of interest in this work, the CA (or the tracer) cannot diffuse into the cells. The rates of the exchange between the two compartments are denoted by the PK parameters K^{trans} and k_{ep} . This is clearly illustrated in Figure 1.

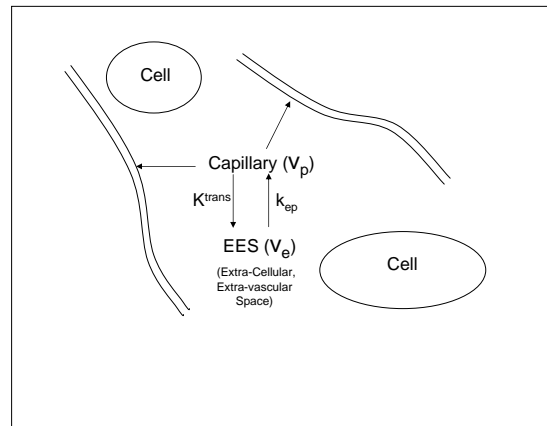


Figure 1. Microscopic View of Tofts' Two-compartment model

This model is chosen for its relative simplicity among compartmental models and over heuristic models since it describes the physical behavior of the underlying structure and is hence more intuitive. It starts from the differential equation describing the exchange of the Contrast Agent (CA) as described in Figure 1 :

$$\frac{dc_e(t)}{dt} = K^{trans} c_p(t) - k_{ep} c_e(t) \quad (1)$$

where K^{trans} quantifies the flow of CA from the plasma to the EES and k_{ep} quantifies the flow of CA from the EES to the plasma. $c_p(t)$ is the Arterial Input Function (AIF) and is the term that represents the CA concentration in the plasma surrounding the EES, which is effectively the 'input' to the EES itself.

The solution for this differential equation is:

$$c_e(t) = K^{trans} c_p(t) * e^{-k_{ep}t} \quad (2)$$

It is important to note that this expression only accounts for the tracer (equivalent to CA) component in the EES itself. In certain scenarios (discussed in detail in [5]), the vascular tracer component cannot be neglected. The extended Tofts model takes this component into account to yield the following expression for the total concentration:

$$c_T(t) = v_p c_p(t) + K^{trans} c_p(t) * e^{-k_{ep}t} \quad (3)$$

The first term denotes the vascular tracer and the second denotes the tracer in the EES as a result of the exchange between the two compartments. The AIF ($c_p(t)$) is unique to each patient and crucial because, as noted previously the tracer concentration in the plasma(explained further in [7]) is the input to the tissue itself.

The different approaches to handle the AIF are outside the scope of this paper. The interested reader is referred to [5]. We are interested in the most generic case where analysis is to be performed in the absence of a measured AIF. In this case, the following model is widely used as a standard AIF(e.g. [4]):

$$c_p(t) = D \sum_{i=1}^2 a_i e^{-m_i t} \quad (4)$$

where D is the dosage per kg body weight, and the a_i s and m_i s are constants that describe the bi-exponential decay of the AIF.

The three parameters to be estimated for this original model are :

1. v_p : the plasma volume. This is physically analogous to a volume fraction. (Unit : $A.U.$ (Arbitrary Unit))
2. K^{trans} : measure of the flow of CA from the plasma to the EES. (Unit : $A.U./min$)
3. k_{ep} : measure of the flow of CA from the EES to the plasma. (Unit : min^{-1})

The use of $A.U.$ in the units for the above quantities is because, though the model is defined on concentration, in practice, we fit it to the observed signal intensity. This same implementation detail also accounts for why the values don't meet the exact conditions outlined in [5]. For example, though K^{trans} is ideally expected to be much smaller in value than k_{ep} , we have generally observed the opposite to be true. Thus, the volume fraction v_e that we actually compute will be greater than 1 (and it will be in units of $A.U.$ rather than dimensionless).

2.2. Role of Arterial Input Function in Pharmacokinetic (PK) Analysis

In compartmental models, PK analysis models the interaction between the compartments or sections of the anatomical structure under study. While these models are theoretically superior to heuristic models in describing the underlying anatomy, the disadvantage is that the 'input' to these structures needs to be known apriori. It is simply the CA concentration in the blood being fed to the first compartment in the model, and is referred to as the Arterial Input Function (AIF). As is obvious from the equations for the Tofts model, the accuracy in estimating the AIF directly affects the accuracy of the estimated PK parameters. The primary difficulty is, however, in measuring this quantity reliably, and this motivates an entire family of approaches that attempt to analytically eliminate the AIF from PK analysis or to circumvent its estimation by other means. The category of approaches that use data from other regions within the image towards the AIF are typically referred to as Reference Region approaches and are discussed in the next section. The compartmental approach and the role of the AIF can be found in greater detail in [2], [3] and [6].

2.3. Reference Region approaches

The basic assumption behind Reference Region (RR) approaches to pharmacokinetic (PK) analysis is that all regions within a given image have the same Arterial Input Function (AIF) if the effects of differences in dispersion are neglected. The approach then is to relate the concentration at the region being analysed to that of a reference region, and to eliminate the AIF between the two expressions. The proposed framework is derived starting from a similar premise. However, the formulation is such that the PK analysis can be

performed in a different parameter space, with no assumptions of the parameters for the reference region, while simultaneously ensuring that with appropriate choice of the reference region, the PK parameters are naturally normalized so that data from different patients can be compared, making population studies feasible.

3. PROPOSED MODEL

The proposed model uses Tofts model to describe concentration at each voxel with respect to the true AIF for the case, and subsequently eliminates AIF by directly relating concentration at the voxel being analysed to the reference voxel concentration.

3.1. Derivation of model equation

Using Tofts model, we write the expressions for the concentration at the analysed and reference voxels as follows:

$$c_T(t) = v_p c_p(t) + K^{trans} c_p(t) * e^{-k_{ep}t} \quad (5)$$

$$c_R(t) = v_p^R c_p(t) + K^{transR} c_p(t) * e^{-k_{ep}^R t} \quad (6)$$

Here, $c_T(t)$ denotes the concentration at the voxel being analysed, $c_R(t)$ denotes the concentration at the reference voxel, $c_p(t)$ denotes the true AIF, v_p , K^{trans} and k_{ep} are the Tofts model parameters for the voxel being analysed, v_p^R , K^{transR} and k_{ep}^R are the Tofts model parameters for the reference voxel.

Applying the Laplace transform to equations (5) and (6), we obtain

$$C_T(s) = v_p C_p(s) + K^{trans} C_p(s) \frac{1}{s + k_{ep}} \quad (7)$$

and

$$C_R(s) = v_p^R C_p(s) + K^{transR} C_p(s) \frac{1}{s + k_{ep}^R} \quad (8)$$

where $C_T(s)$, $C_R(s)$ and $C_p(s)$ are the laplace transforms of $c_T(t)$, $c_T(t)$ and $c_p(t)$ respectively.

Dividing 7 by 8 and simplifying using partial fractions, we get

$$\frac{C_T(s)}{C_R(s)} = \frac{A_1}{s + B_1} + \frac{A_2}{s + B_2} + A_3 \quad (9)$$

where

$$\begin{aligned} A_1 &= \frac{K^{transR}}{v_p^R(k_{ep} - k_{ep}^R) - K^{transR}} \frac{v_p(k_{ep}^R v_p^R + K^{transR}) - v_p^R(k_{ep} v_p + K^{trans})}{v_p^{R2}} \\ B_1 &= k_{ep}^R + \frac{K^{transR}}{v_p^R} \\ A_2 &= \frac{(k_{ep}^R - k_{ep})K^{trans}}{v_p^R(k_{ep}^R - k_{ep}) + K^{transR}} \\ B_2 &= k_{ep} \text{ and } A_3 = \frac{v_p}{v_p^R} \end{aligned} \quad (10)$$

Taking the inverse Laplace transform, we obtain the expression for the current voxel's concentration time series in terms of that of the reference voxel as

$$c_T(t) = (A_1 e^{-B_1 t} + A_2 e^{-B_2 t}) * c_R(t) + A_3 c_R(t) \quad (11)$$

For the sake of completeness, we also need to consider the case of when the transfer function has repeated poles. This is the case when the following condition holds.

$$k_{ep}^R + \frac{K^{transR}}{v_p^R} = k_{ep} \quad (12)$$

In this special case, by a similar approach using the laplace tranform and the partial fractions simplification, we obtain the following transfer function:

$$\frac{C_T(s)}{C_R(s)} = \frac{C_1 s}{(s + B)^2} + \frac{C_2}{(s + B)} + C_3 \quad (13)$$

where

$$\begin{aligned} C_1 &= -\frac{K^{trans}(k_{ep}^R - k_{ep})}{v_p^R \cdot k_{ep}}, \\ C_2 &= \frac{v_p}{v_p^R k_{ep}} \left[\left\{ k_{ep} + \frac{K^{trans}}{v_p} \right\} k_{ep}^R - k_{ep}^2 \right] \\ C_3 &= \frac{v_p}{v_p^R} \\ B &= k_{ep}^R + \frac{K^{transR}}{v_p^R} = k_{ep} \end{aligned} \quad (14)$$

Taking the inverse laplace transform, we obtain the following expression relating the current voxel's concentration to that of the reference region:

$$C_T(t) = C_1(Bt + 1)e^{-Bt} * C_R(t) + C_2 e^{-Bt} * C_R(t) + C_3 C_R(t) \quad (15)$$

3.2. Justification for proposed model

Viewing anatomical structures as filters, we can denote the responses for the reference and analysis regions in different images. Let us consider two images I_1 and I_2 (i.e., from different patients). Let H_1 denote the filter response of the reference region in I_1 , and Q_1 denote the filter response of the analysed region in I_1 . Similarly, let H_2 and Q_2 denote the filter responses of the reference region and analysis region respectively, in I_2 .

To correlate with the original PK coefficients, Q_i is analogous to v_p^i , K^{trans^i} and k_{ep}^i , where the latter are the PK coefficients for the analysed voxel in I_i when $i=1,2$ etc. PK analysis compares Q_1 and Q_2 . The proposed approach amounts to comparing $H_1^{-1}Q_1$ and $H_2^{-1}Q_2$. Since the RRs are assumed to be the same structure from different images, $H_1 = H_2$. Thus, the two frameworks yield the same effective comparison. (See Figure 2 for the anatomical and filter views.)

3.3. Uniqueness of the proposed approach

The work in [7] clearly explains the significance of the AIF and the goal of RR approaches with regards to AIF elimination. The proposed framework differs from existing RR approaches (e.g. [7]) in certain key aspects. It is based on the extended model accounting for the vascular CA component and is thus more generic. Also, we do not need to assign the values of the PK parameters of the reference region. Additionally, the structure of the proposed model is such that no additional measurements or calibration are needed in MR acquisition.

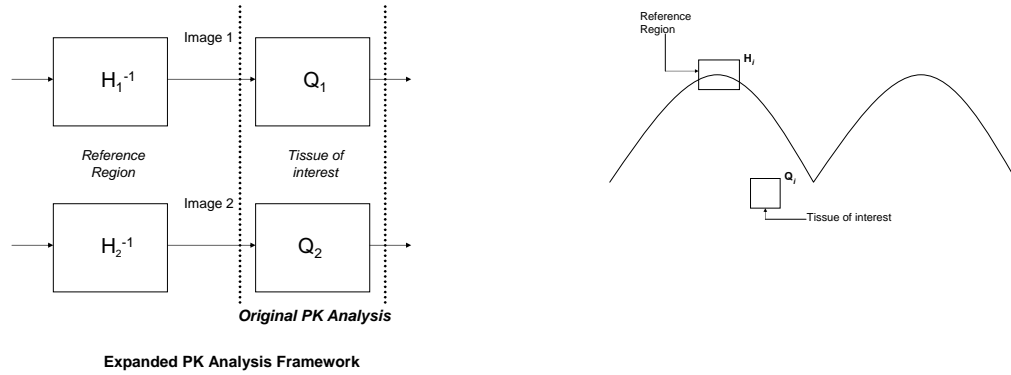


Figure 2. Justification of the proposed model

3.4. Potential sources of error in the proposed model

It is important to note that the proposed model – like all PK models – describes the time-evolution of CA concentration. However, in DCE-MRI, the concentration is not directly accessible and instead, observed signal intensities are related to it nonlinearly. The linear approximation employed in the process of fitting the signal intensities to the derived relationships, could be a potential source of error for the proposed framework. In theory, we could account for the analytic relationship between intensity and CA concentration and write the model directly in terms of intensities. However, this would lead to a more complicated model and hence increase computation requirements. Hence, the extent of this effect is first being studied through experiments. Also, the extent of normalization achieved is sensitive to how consistently the RR can be chosen over images.

4. IMPLEMENTATION AND EXPERIMENTS

In this work, the conjugate-gradient technique was chosen to estimate the parameters of the enhanced model. Also, in looking at the expressions for the parameters, we observe that B_1 is only dependent upon the original (Tofts model) PK parameters of the RR. This implies that by definition, this quantity is expected to be the same for all the voxels in the given image. Thus, in our implementation, we constrain B_1 to be same across all the voxels of an image as well as across images. An automatic module for the nipple detection in [1] was used. The technique was tested over a population comprising 40 data sets, each from a different patient. Candidate lesions within each data set were made available through a semi-automatic segmentation of the 20 largest lesions in each data set, and this was used to evaluate the performance of the proposed framework by comparison to the ground truth. Also, the parameter distribution within lesions for all these cases was studied to identify patterns that could be used to distinguish malignant and benign lesions.

Note that the special case of the repeated poles in Equation 15 is mentioned in this paper for completeness. In practice, it is not possible to know apriori which model should be fit to the data being analysed since that would require knowledge of the parameters of the Tofts model itself. A simple solution would be to attempt to fit both models to each voxel and pick the one with lower value of error. However, due to the increased computational burden that this would present, we chose to fit the general model as given in Equation 9 everywhere.

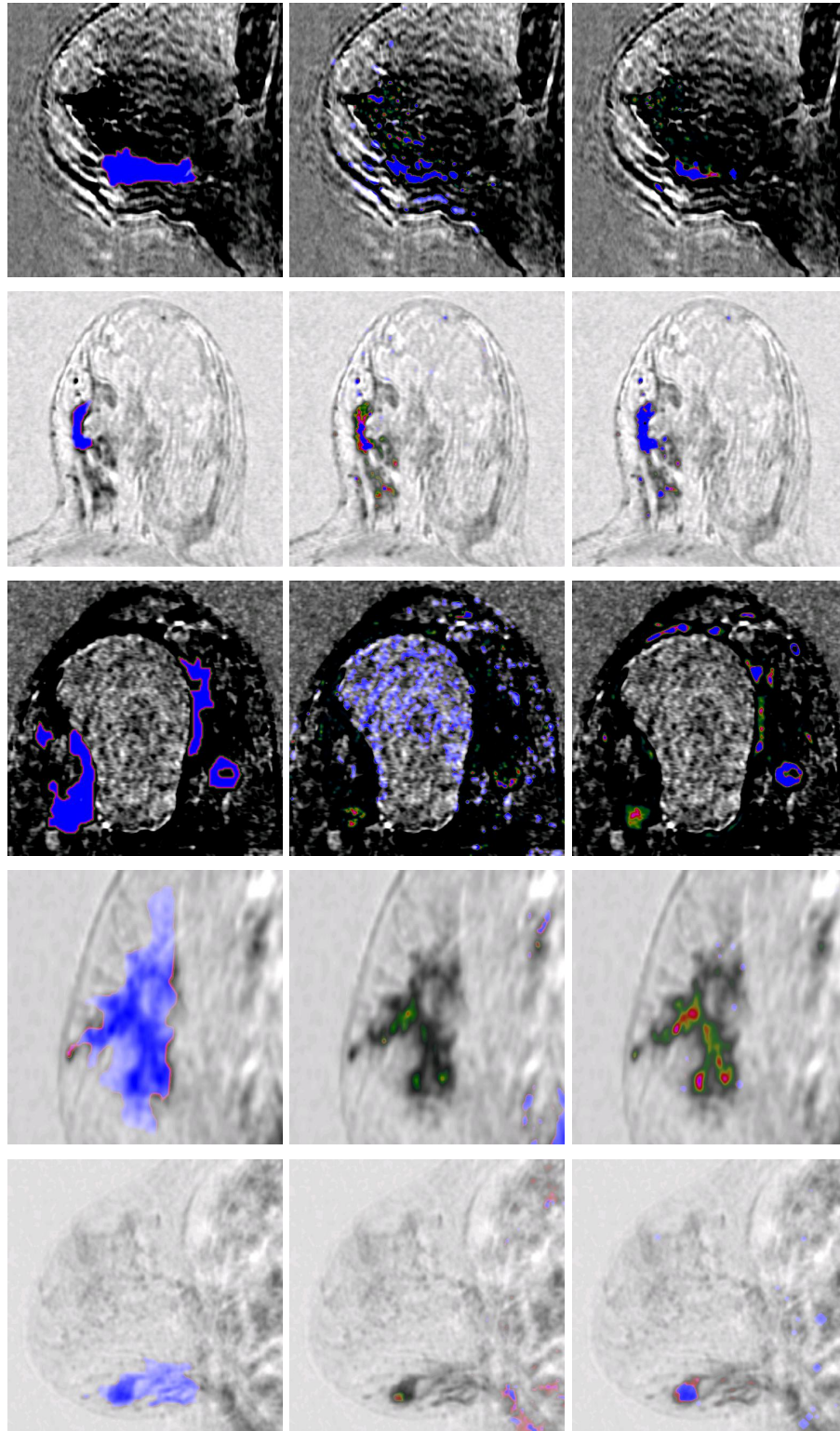


Figure 3. Results comparing the manually segmented ground truth (Column 1) with results from Tofts Model (Column 2) and the Proposed model (Column 3). Note the improved localization of regions of interest, and the reduction in false positives.

5. RESULTS

Figure 3 shows the results of the experiments comparing pharmacokinetic analysis using Tofts model with the proposed model. All five cases included here were malignant. Column 1 indicates the ground truth, while Columns 2 and 3 show the regions of interest as localized by analysis using the Tofts model and the proposed model respectively. The data in these figures (on which the localized regions of interest are superimposed in color with blue being the highest in value) is inverted so that in interpreting these figures, darker regions indicate greater enhancement and brighter regions indicate lesser enhancement. The lesion localization and lesion areas as indicated in these images can be directly compared to compare the performance of the two models.

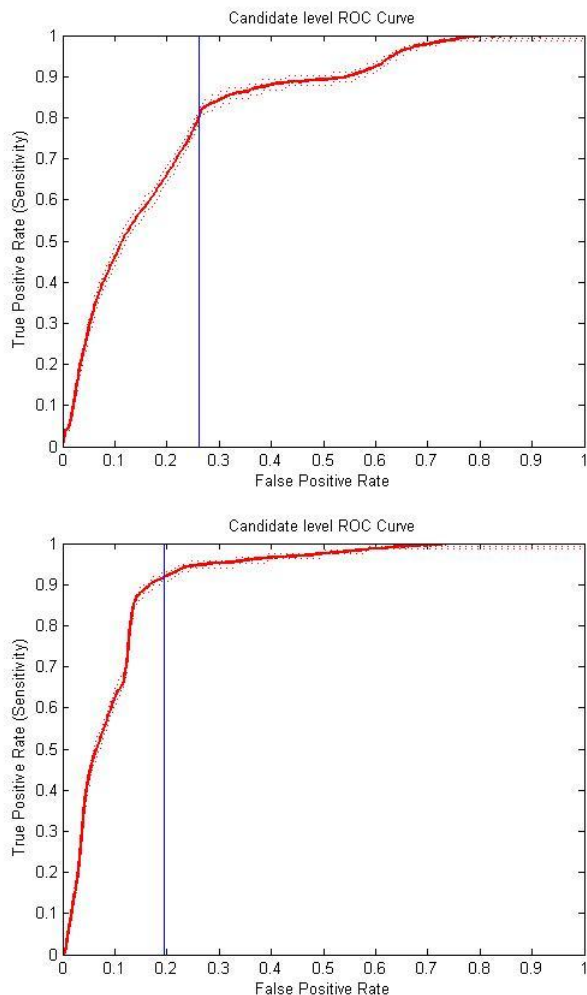


Figure 4. ROC curves for (a) Tofts Model, (b) Proposed Model

5.1. Observations

The estimated parameters for the proposed five-parameter model are observed to be better correlated across different patients than the original Tofts parameters as estimated with the standard AIF. However, the parameters are sensitive to the RR chosen and hence the extent of normalization across patients is dependent on how consistently the RR is chosen across images. The current RR of choice is the nipple region. The main reasons for this choice are that the enhancement characteristics of the nipple are relatively

similar across images and also that the nipple is a relatively clear structure and easy to automatically locate in the breast MR. An alternate choice for the RR would be the pectoral muscle. It would be interesting to use the pectoral muscle for the RR and compare the results obtained with those from the current work. It is also important to note that there are breast MR images in which the nipple is not clear or not seen or in cases of lumpectomy, the nipple might be missing in which case a structure like the pectoral muscle might prove more reliable as a RR.

As is clear in Figure 3, visually the proposed model localizes the malignant lesions better than the analysis that uses the Tofts model with a standard AIF. Also, the number of false positives or spurious voxels picked up is far lesser for the proposed model. These two aspects clearly demonstrate the effectiveness of the proposed model in visually highlighting suspicious voxels for further analysis by radiologists. In order to better understand the performance of the proposed model in population studies, both the proposed framework and the framework based on the Tofts model were applied to all 40 data sets. The results from classification using both approaches were compared using Receiver Operating Characteristics (ROC) curves. These are shown in Figure 4. These clearly indicate that the proposed model allows better classification than the extended Tofts model, in the sense of yielding higher sensitivity than the latter at comparable discrimination thresholds. This clearly illustrates the potential for the proposed model in population studies. It is also expected that with more robust RR selection and more accurate model fitting, the classification accuracy obtained with the proposed model can be improved further.

6. CONCLUSIONS AND FUTURE WORK

The work discussed in this paper proposes an enhanced model for pharmacokinetic analysis based on the Tofts model. The new model offers the advantages of eliminating the estimation of the AIF, and normalizing the resulting parameters so as to facilitate population studies. In our experiments across 40 patients, the estimated parameters for the proposed model displayed greater correlation across patients than did the Tofts model parameters (with standard AIF). Also, on visual inspection and by thresholding, the results from the enhanced model were less noisy while still capturing most of the lesion area which is very promising.

Since the enhanced model parameters are functions of those of the Tofts model at the voxels being analysed and used for reference, it is theoretically possible to estimate the Tofts model parameters without the AIF estimation or to directly estimate the AIF for any subsequent analysis by using the proposed framework. Using this framework on a pair of voxels yields five parameters that are functions of the original PK parameters (three each) of the two individual voxels. Using v voxels, there would be $3v$ unknowns and $5\frac{v(v-1)}{2}$ equations. Solving the inequality, we see that three or more voxels will be sufficient for solving for the individual PK parameter values. We can then use the CA time-series and PK parameters to estimate the AIF itself.

Our experiments so far indicate great potential in the proposed model and validate it for population pharmacokinetic studies. It is of interest to test this framework on larger data sets as well as on unseen data, to study how effective the normalization is and how sensitive it is to the choice of reference region. It is also of interest to understand the physical significance of the enhanced model parameters by studying their relationships to the Tofts model parameters whose physical significance is understood. The frameworks for AIF estimation and Tofts model parameter estimation are currently being pursued.

References

- [1] Mert Dikmen, Yiqiang Zhan, and Xiang Sean Zhou. Joint Detection and Localization of Multiple Anatomical Landmarks through Learning. *SPIE Medical Imaging*, 2008.
- [2] R.E. Port, M.V. Knopp, U. Hoffmann, S. Milker-Zabel, and G. Brix. Multicompartment analysis of gadolinium chelate kinetics: Blood-tissue exchange in mammary tumors as monitored by dynamic MR imaging. *Journal of Magnetic Resonance Imaging*, 10(3):233–241, 1999.

- [3] NE Simpson, Z. He, and JL Evelhoch. Deuterium NMR tissue perfusion measurements using the tracer uptake approach: I. *Optimization of methods. Magn Reson Med*, 42:42–52, 1999.
- [4] R. Srikanchana, D. Thomasson, P. Choyke, and A. Dwyer. A comparison of pharmacokinetic models of dynamic contrast-enhanced MRI. *CBMS 2004. Proceedings. 17th IEEE Symposium on Computer-Based Medical Systems, 2004.*, pages 361–366, 2004.
- [5] PS Tofts, G. Brix, DL Buckley, JL Evelhoch, E. Henderson, MV Knopp, HBW Larsson, TY Lee, NA Mayr, GJM Parker, et al. Estimating kinetic parameters from dynamic contrast-enhanced T1-weighted MRI of diffusable tracer: a common global language for standardized quantities and symbols. *J Magn Reson Imaging*, 10:223–232, 1999.
- [6] HJ Weinmann, M. Laniado, and W. Mützel. Pharmacokinetics of GdDTPA/dimeglumine after intravenous injection into healthy volunteers. *Physiological chemistry and physics and medical NMR*, 16(2):167–172, 1984.
- [7] T.E. Yankeelov, J.J. Luci, M. Lepage, R. Li, L. Debusk, P.C. Lin, R.R. Price, and J.C. Gore. Quantitative pharmacokinetic analysis of DCE-MRI data without an arterial input function: a reference region model. *Magnetic Resonance Imaging*, 23(4):519–529, 2005.